Comet showers as a cause of mass extinctions

Piet Hut*, Walter Alvarez†, William P. Elder‡, Thor Hansen§, Erle G. Kauffman‡, Gerta Keller‖, Eugene M. Shoemaker¶ & Paul R. Weissman#

* The Institute for Advanced Study, Princeton, New Jersey 08540, USA
† Department of Geology and Geophysics, University of California, Berkeley, California 94720, USA
‡ Department of Geological Sciences, University of Colorado, Boulder, Colorado 80309, USA
§ Department of Geology, Western Washington University, Bellingham, Washington 98225, USA
‖ Department of Geological and Geophysical Sciences, Princeton University, Princeton, New Jersey 08540, USA
¶ Branch of Astrogeology, US Geological Survey, Flagstaff, Arizona 86001, USA
# Earth and Space Sciences Division, Jet Propulsion Laboratory, Pasadena, California 91109, USA

If at least some mass extinctions are caused by impacts, why do they extend over intervals of one to three million years and have a partly stepwise character? The solution may be provided by multiple cometary impacts. Astronomical, geological and palaeontological evidence is consistent with a causal connection between comet showers, clusters of impact events and stepwise mass extinctions, but it is too early to tell how pervasive this relationship may be.

BRIEF intervals of greatly increased impact frequency must have occurred on Earth during occasional comet showers. Such showers are caused by perturbations of the Oort comet cloud due to close passages of neighbouring stars. Here we explore the hypothesis that these comet showers may have caused stepwise mass extinctions through multiple impacts within a short period of time. This hypothesis is based on calculations of orbital dynamics, age data on terrestrial impact craters, and the stratigraphic record of impact and extinction events. We do not maintain that this hypothesis has been demonstrated to be correct, only that there is enough evidence that it must be taken seriously and should be carefully tested.

Impacts of Earth-crossing asteroids take place randomly in time[1]. A significant fraction of comets, however, should arrive in discrete showers triggered by a relatively close passage of a star or interstellar gas cloud[2]. Early calculations[2,3] indicated that such comet showers should last ~1 Myr. We present a detailed calculation of the temporal profile of such a comet shower, which turns out to last ~3 megayears, with the bulk of the comets arriving within ~1 Myr.

A number of geological and palaeontological observations suggest that such showers have occurred: clustered crater ages, stratigraphic horizons of impact ejecta closely spaced in time, and evidence for three stepwise mass extinctions spanning intervals of 1-3 Myr during the past 100 Myr, corresponding to the Eocene/Oligocene (E/O), Cretaceous/Tertiary (K/T) and Cenomanian/Turonian (C/T) boundary zones. This tentative evidence warrants further investigation.

In 1980, Alvarez *et al.*[4] presented evidence that the end-Cretaceous mass extinction was caused by a large impact. Abundant supporting evidence comes from studies of the Cretaceous/Tertiary boundary focusing on iridium content[5,6], osmium isotopes[7], the chemistry and mineralogy of the boundary clay[8], spherules of possible impact-melt origin[9-11], shocked mineral grains[12-14], soot particles[15], and the mechanism needed to distribute boundary materials worldwide[16]. Alternative viewpoints[17-22] have been debated in the literature[23,24]. The late Eocene mass extinction (~36-40 Myr BP) also displays evidence for one or more impacts[25-38].

Some palaeontologists have argued that the end-Cretaceous mass extinction took place gradually over a few million years[39], but the relevant fossil record is complex[24,40]. Dinosaur fossils are too rare to determine whether their extinction was abrupt or gradual. Some invertebrates (such as ammonites and rudists) were seriously depleted 1-2 Myr before the end of the Cretaceous. Other invertebrates (bivalves, brachiopods, bryozoa and foraminifera) and the coccoliths were decimated abruptly, during an interval of evolutionary diversification, at precisely the time of the K/T impact.

Fischer and Arthur[41] first suggested that mass extinctions might occur periodically; Raup and Sepkoski[42] presented quantitative palaeontological support for a 26-Myr extinction periodicity. To explain periodic mass extinctions, two of which roughly coincided with major impacts, a mechanism for producing periodic impacts was needed. Hills[2] showed that disturbances of the Oort cloud could produce comet showers and clustered impacts, and suggested a relation between this mechanism and the end-Cretaceous mass extinction. Independently, Davis *et al.*[43] and Whitmire and Jackson[44] proposed periodic disturbances of the Oort cloud by a distant companion star of the Sun, and Rampino and Stothers[45] suggested that the disturbances result from oscillations of the Solar System through the galactic plane.

The evidence for periodicity was hotly debated, but a realization emerged that non-periodic comet showers resulting from encounters with passing stars should also be considered, as in Hills' original suggestion. Muller[3,46] first noted that a mass extinction occurring as the result of multiple impacts during a comet shower might take place in discrete extinction steps and thus be confused with a gradual extinction. Meanwhile, the concept of stepwise mass extinctions was independently developed from high-resolution stratigraphic studies—by Kauffman[47-49] for the Cretaceous/Tertiary and Cenomian/Turonian mass extinctions, by Keller[32-34] for the late Eocene extinctions, and by Raup[50], who used the taxonomic data base of Raup and Sepkoski[42,51]. Evidence for multiple impacts in the Late Eocene[45,52], and hints of clustering in time of impact crater ages[53], strengthened the case for comet showers. Somewhat later, another scheme for explaining periodic comet showers was proposed, based on an as yet unobserved Planet X[54], but this model seemed to be inconsistent[55].

Our purpose here is partly to review the literature bearing on the hypothesized relationship between comet showers and stepwise mass extinctions, and partly to summarize the results of our investigations of this hypothesis during the past two years.

Astronomical theory of comet showers

Although the original impact explanation for the iridium anomaly at the K/T boundary term was termed "the asteroid-impact hypothesis", it was realized that a comet impact would provide an equally plausible explanation for the observed iridium excess. It is not easy to decide which explanation is more likely, as the non-volatile component of comets probable has a chemical composition close to that of the primitive car-

bonaceous chondrites[56]. As comets probably consist of a roughly equal mixture of silicates, hydrocarbons and volatile ices, their expected bulk iridium content is somewhat less than one-third that of an undifferentiated carbonaceous asteroid. Another difference is that long-period comets typically strike the Earth at about three times the velocity of asteroids, and therefore impart an order of magnitude more energy than an asteroid of comparable mass.

There is little specific evidence to distinguish between a cometary or an asteroidal impactor at the K/T boundary. Palme[57] has argued that the siderophile signature in the boundary clay "does not match ... the pattern of unfractionated meteorites (chondrites)," and an iron-asteroid impactor has been suggested. Asaro[58], on the other hand, considers that the elemental ratios in the boundary clay do match CI carbonaceous chondrites.

Asteroids are expected to collide with the Earth at essentially random intervals, with an expected half-life for Earth-crossing asteroids of ~30 Myr (ref. 1). Some Earth-crossing asteroids may be derived from short-period comets, so their population and flux may be modulated by comet showers. We might expect each comet shower to be followed by an extended tail of impacts by asteroids derived from short-period comets. But these (possibly overlapping) tails may be difficult to discriminate from the steady-state flux of long-period comets and Earth-crossing asteroids. In the calculations of the temporal profile of a comet shower we can safely neglect the small contribution of comets-turned-asteroids, at least for the major part of the shower.

Comets are also expected to collide with the Earth at random times, arriving from the outer Oort cloud (from distances of $>2\times10^4$ astronomical units (AU)), where the perturbations by the galactic tides[59] and the frequent perturbations by passing stars provide a trickle of new comets into the planetary region. On rare occasions, the passage of a star close to the Sun, or a close passage by a massive interstellar gas cloud, will significantly perturb the inner Oort cloud as well. This region is expected to contain a much higher density of comets than the outer Oort cloud (refs 2, 60, 61 and M. Duncan, T. Quinn and S. Tremaine, preprint). Any perturbation of this inner region that fills the loss cone will cause a comet shower to occur throughout the inner planetary region, within one orbital period of the comets in the inner Oort cloud (ref. 62 and J. Heisler, S. Tremaine and C. Alcock, preprint).

On entering the inner planetary system, the orbital semi-major axes (and thus the orbital energies) of the comets are strongly perturbed by Jupiter and Saturn, so that most are removed or 'lost' from the Oort cloud (hence the names 'loss cone' or 'loss cylinder' for the region in velocity space within which the orbits pass through the inner planetary system). Weissman[63-64] showed that a typical Oort-cloud comet (semi-major axis 2.5×10^4 AU) passing within the orbit of Jupiter would either be ejected from the Solar System on a hyperbolic orbit or captured to a shorter-period orbit where stellar perturbations were not important, with <5% of the comets returning to the outer Oort cloud. Weissman found that the average long-period comet made only five perihelion passages, with an average time of 6×10^5 yr between the first and last passage. Of the long-period comets, 65% were ejected, 27% randomly disrupted and 8% lost to a variety of lesser end-states, such as sublimation of all volatiles or perturbation to a Sun impacting orbit. A very small fraction of the long-period comets, on the order of 4×10^{-4}, evolved to short-period orbits (periods <200 yr) after an average of almost 400 returns. The short-period comets return frequently to the planetary region until they are ejected by perturbations caused by Jupiter (on a timescale of ~1 Myr), totalty disintegrate (after several thousand returns) or evolve both physically and dynamically to asteroidal objects in Earth-approaching orbits.

Comets perturbed into the planetary region in a comet shower from the inner Oort cloud would be expected to behave similarly to the long-period comets described above, except for the effect of their small initial orbital semi-major axes. We have studied

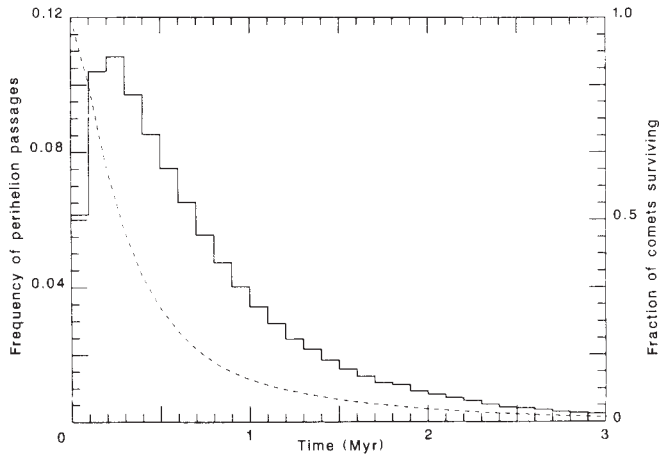

Fig. 1 Profile of a comet shower caused by an instantaneous perturbation. The dashed line shows the rapidly falling fraction of surviving comets; that is, comets that are neither being thrown out of the inner Oort cloud by planetary perturbations, nor are destroyed by physical mechanisms such as break-up or sublimation. The solid line indicates the frequency of perihelion passages, which measures the probability of an impact on Earth.

the evolution of a cometary shower in time using Weissman's[63,64] Monte Carlo simulation model for the long-period comets. In doing so we have assumed that comets in the inner and outer Oort cloud are physically similar, in that their sublimation lifetime, probability of random disruption, and propensity for forming non-volatile crusts are the same. In our simulation we started 5×10^6 comets in orbits with orbital energies uniformly spread between semi-major axes of 3×10^3 and 10^4 AU, perihelia uniformly spread between 0.01 and 4.0 AU, and initial orbital phases spread uniformly in mean anomaly. It was found that the average Earth-crossing comet made 8.6 returns to the planetary region, with an average lifetime of 0.48 Myr. The largest fraction of comets, 63%, were ejected by Jupiter perturbations, 31% were lost to random disruption and 5% had their perihelia perturbed out of the planetary region to orbits in the outer Oort cloud.

Figure 1 shows the number of comets surviving in the system with time (dashed line). The number initially declines rapidly, with a half-life of <0.3 Myr. Also shown (solid line) is the number of perihelion passages versus time. This curve rises quickly as comets begin arriving in the planetary region on their long-period orbits. It declines less rapidly because, although the number of comets is monotonically decreasing, the orbital periods of the surviving comets are also decreasing, leading to more frequent perihelion passages for each survivor. Thus, a small fraction of the comets in the system accounts for a large fraction of the later cometary returns.

The peak of the distribution for the number of perihelion passages versus time (Fig. 1) has a full-width at half-maximum (FWHM) of 0.8 Myr. The times after the initial perturbation for 25, 50 and 75% of the perihelion passages to have occurred are 0.3, 0.5 and 0.9 Myr, respectively. More than 90% of the returns occur in the first 1.8 Myr after the perturbation of the Oort cloud and 99% in 4.0 Myr.

The shapes of the two curves described above are relatively insensitive to the physical and dynamical parameters that enter the Monte Carlo simulation. Variations in the disruption probabilities, sublimation lifetimes or orbital energy distribution in the inner Oort cloud do not change the peak flux or shower duration by more than 20%. This result was confirmed by running the Monte Carlo simulation while varying the model parameters. Weissman's simulation model has already been 'tuned' to mimic the evolution of the observed long-period comets; substantial changes of parameters outside the ranges studied would result in disagreement with observed cometary

behavior. After finishing these calculations, we learned that Fernández and Ip[62] report similar calculations, consistent with Fig. 1.

If the perturbing force is due to the distant passage of a massive interstellar gas cloud rather than a close stellar encounter, the resulting disturbance will be spread over ~1 Myr, and will broaden the distribution of arrival times to a FWHM of ~1.5 Myr. A star passing at a distance of 10,000 AU and traveling at 40 km s^{-1} perturbs the inner Oort cloud during an interval of only ~0.01 Myr; an interstellar gas cloud (or subcondensation within a larger gas cloud) passing at 10 parsecs with a relative speed of 20 km s^{-1} exerts a significant perturbation during ~1 Myr. Alternatively, if the Sun has a companion star which traverses the inner Oort cloud every ~26–28 Myr[43,44,65,66], the duration of the perturbation can be similarly extended.

It is difficult to assess the exact number of comets in a shower, as that figure will be sensitive to the population of comets in the inner Oort Cloud as well as the velocity, mass and encounter distance of the passing star. Heisler *et al.* (J. Heisler, S. Tremaine and C. Alcock, preprint) have shown that even the flux of comets from the outer Oort cloud can easily vary by a factor of 3–5 owing to random stellar perturbation. Thus, whereas current estimates place comets as accounting for ~50% of the steady-state cratering on the Earth[67], the true fraction may be considerably different if the current short-term estimates of the cometary flux are different from the true long-term average. Taking current best-guesses for the relevant parameters (but keeping in mind the factor of 3–5 additional uncertainty), we estimate that a major cometary shower involving ~10^9 comets of >3 km diameter perturbed into Earth-crossing orbits would result in ~20 impacts, and would occur every 300–500 Myr. Minor showers involving ~10^8 comets and ~2 such impacts would occur more frequently, every 30–50 Myr.

The conclusions useful for a comparison with possibly related terrestrial geological phenomena are as follows: (1) the time spans of clustering of terrestrial phenomena should be comparable to that shown in Fig. 1; (2) if the distribution roughly corresponds to that in Fig. 1, but is somewhat broader, the cause could be a comet shower involving comets in somewhat more distant orbits in the Oort cloud, or it could indicate a triggering by the passage of a companion star or a massive distant object such as an interstellar gas cloud; (3) if the distribution is spread out over a length of time much larger than that shown in Fig. 1, it is unlikely that a single comet shower can explain the events; (4) similarly, if the distribution of possibly impact-related phenomena exhibits a significantly shorter duration than that shown in Fig. 1, a comet shower cannot explain the events.

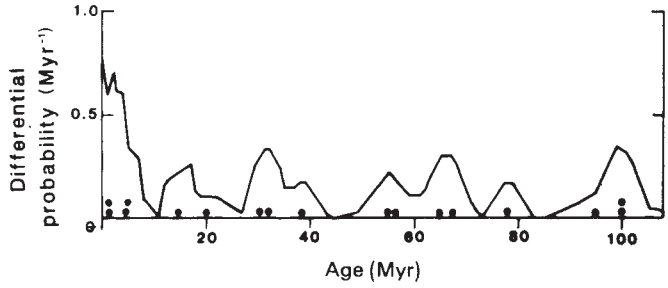

Fig. 2 Smoothed probability distribution of ages of observed terrestrial impact structures during the last 100 Myr, derived from ages presented in ref. 52. The probability distribution has been smoothed by a 6-Myr running mean. Dots represent central values of estimated ages.

Geological observations of impact events

Seventeen terrestrial impact structures are known with mean diameters of ≥5 km and for which the best estimated ages are <100 Myr and are thought to have an uncertainty (1σ) less than ±15 Myr[68].

Figure 2 shows a probability distribution of age for these structures, obtained by smoothing with a 6-Myr running mean the probability distribution for each impact structure, represented by a box of width 2σ[68]. Four peaks rise above the rest in the distribution, one crowded against the present, a second centred near 35 Myr, a third near 65 Myr and a fourth near 99 Myr.

It should be kept in mind that the moderately well dated impact structures are only a small sample of all the impact structures that have probably been formed on the continents in the past 100 Myr. Most distributions of 17 ages drawn at random from a uniformly distributed population of ages would have peaks similar in magnitude or larger than those centred at 35, 65 and 99 Myr. It may be significant, however, that the largest Phanerozoic impact structure so far discovered corresponds to one of the events in the broad peak centred at 35 Myr, and that the age of the impact event recorded by the noble-metal-bearing clay layer at the Cretaceous/Tertiary boundary coincides with the center of the 65 Myr peak.

Table 1 Ages of strewn fields of impact glass*

	Dating method	Age (Myr)	Reference
Indochinites and philippinites (includes microtektites)	^{40}Ar-^{39}Ar	0.690 ± 0.028†	71
	Fission track	0.693 ± 0.025	70
Darwin glass	K-Ar	0.70 ± 0.08	
	Fission track	0.74 ± 0.04	118
Australites	Fission track	0.830 ± 0.028	70
	K-Ar	0.86 ± 0.06	119
	^{40}Ar-^{39}Ar	0.887 ± 0.034	71
Irgizites‡	Fission track	1.07 ± 0.06	120
Ivory Coast tektites§ (includes microtektites)	Fission track	1.08 ± 0.10	121
South Australian high-Na tektites	Fission track	≥8.55 ± 0.90	122
Moldavites‖	Fission track	14.7 ± 0.4	121
Libyan Desert glass¶	Fission track	29.4 ± 0.5	121
North American tekites (includes microtektites)	Fission track	34.6 ± 0.7	121
	Stratigraphic	36.0 ± 0.5	75
Clinopyroxine-bearing micro spherules and microtektites in *Globorotalia cerroazulensis* zone	Stratigraphic	36.4 ± 0.5	75
Cryptocrystalline micro spherules and microtektites in *Globigerapsis semiinvoluta* zone	Stratigraphic	36.4 ± 0.5	75

* Objects which may once have been glass but are no longer glassy, such as spherules found in the clay at the K-T boundary[60] are not included.
† Errors quoted are standard deviations.
‡ Associated with Zhamanshin crater, USSR. ‖ Associated with Ries crater, West Germany.
§ Associated with Bosumtwi crater, Ghana. ¶ Apparently associated with Oasis crater, Libya (undated).

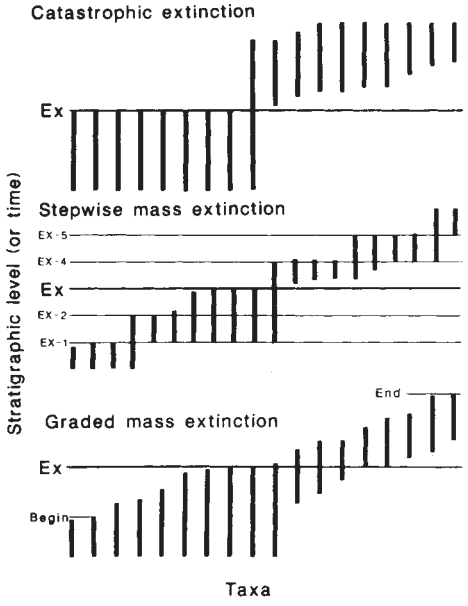

Fig. 3 Models of extinction patterns of taxa (vertical lines) within the framework of the three major theories for mass extinction. 'EX' represents the stratigraphic level (or time) of either maximum taxonomic loss or of the extinction of certain characteristic taxa (such as biostratigraphic indices). EX-1, EX-2, for example, define stepwise extinction events as components of a single mass extinction interval[49].

A variety of impact-formed glasses constitute additional sources of evidence for the times of impact events (Table 1). In three cases, well dated glasses can be correlated with well dated impact craters, but for the remainder of the cases the ages of the glass represent an independent data set. Two clusters of ages are found for the impact glasses, one near 1 Myr and one centred at ~35 Myr, which fall on the two broad peaks of Cenozoic crater ages.

For many years it was generally believed that the tektites found distributed across Southeast Asia, the Philippines, Indonesia and Australia, as well as microtektites widely distributed in deep-sea deposits in the Indian Ocean, belong to a single strewn field, commonly referred to as the Australasian strewn field[69] Recently, Storzer and Wagnet[70] presented new high-precision fission-track ages which suggest that the tektites found in Australia (australites) may be ~0.14 Myr older than the Southeast Asian and Philippine tektites. The apparent difference in the ages has been supported by two new ^{40}Ar–^{39}Ar ages[71]. If this difference is real, the Australasian tektites comprise two major strewn fields that may be partly overlapping. However, a careful search in deep-sea sediments has revealed only one clear-cut layer in the stratigraphic distribution of the microtektites[72]. Two other strewn fields of impact glass, one of which includes the Ivory Coast microtektites, are ~0.2 Myr older than the australites.

Of particular interest is the close spacing of ages of three strewn fields of impact glass in the late Eocene. Two closely spaced layers of microspherules are found in deep-sea sediments in the late Eocene *Globorotalia cerroazulensis* foraminiferal zone. The microspherules in the uppermost layer are crystal-free siliceous microtektites, which are closely similar in chemical and isotopic composition to the North American tektites[25,26]. The tektites and correlated microtektites are distributed over part of North America, the Gulf of Mexico, the Caribbean region and the western North Atlantic[26-29]. Cryptocrystalline and crystal-bearing glass spherules more basic in composition than the microtektites occur in a layer a few tens of centimetres below the North American microtektite horizon at several sites in the Gulf of Mexico and the Caribbean[26]. These spherules are also widely distributed in the central Pacific, where they were originally miscorrelated with the North American microtektites[27-31]. A strong iridium anomaly, with a peak iridium abundance of up to 4.1 p.p.b.[35,36] is coincident with this spherule layer[26-29,37]. In Barbados, the stratigraphic position of the clinopyroxene-bearing spherule layer is marked by a moderate iridium anomaly[27-29,38].

Another well-defined late Eocene, microspherule layer has been found in the western Pacific at DSDP (Deep Sea Drilling Program) Site 292 in core 38-2, between 75 and 80 cm depth (see Fig. 5), and possibly in the Indian Ocean at DSDP Site 216[27-29]. This layer occurs in the *Globigerapsis semiinvoluta* zone[27-29,32-34], and has been correlated previously with one or the other of the microspherule layers in the *G. cerroazulensis* zone[26,37]; however, the biostratigraphy demonstrates that it is older than the microspherule layers in the *G. cerroazulensis* zone.

In summary, four weak peaks are observed in the impact crater age distribution in the past 100 Myr; two clusters of ages of impact glass are broadly coincident with the crater-age peaks in the Cenozoic. Represented within the clusters are major strewn fields of glass and microspherules, three of late Eocene age and at least two and possibly three of Quaternary age. The ages of the Quaternary strewn fields of tektites and microtektites are distributed over ~0.4 Myr. The exat time separation of the late Eocene impact glass horizons is not known; for plausible sedimentation rates, deposition of the two most closely spaced glass horizons was probably separated by between ten and a few tens of thousands of years. Deposition of these glass horizons is separated, in turn, by ~0.5–1.0 Myr from the lower glass horizon. The clustering of ages of most of the known glass strewn fields into two compact age groups is unlikely to be the result of events that are randomly distributed in time[68]. A burst or shower of impacts in the late Eocene seems to be indicated, and a burst may have occurred in the Quaternary.

Palaeontological observations of extinctions

A mass extinction annihilates 50–95% of ecologically and genetically diverse lower taxa within 1–3.5 Myr in well-dated extinction events for which closely spaced stratigraphic and taxonomic data exist (C/T, K/T and E/O events)[49]. Published taxonomic and biostratigraphic data support this concept[42]: the 7 Myr average interval of ref. 42 is based on taxonomic data time-averaged to the stage level.

Figure 3 illustrates the three major concepts of mass extinction[49]. In graded mass extinctions, extinction rates are higher than background levels, but taxa disappear randomly throughout this interval, possibly along an ecological gradient from initially stenotopic to more eurytopic groups. This pattern is attributed to accelerated intervals of environmental change resulting from terrestrial causes (such as eustasy or climate), producing global ecological crises. Catastrophic mass extinction theory[4] views global annihilation among genetically and ecologically diverse organisms as occurring near-simultaneously (days to centuries) as a direct or indirect result of enormous perturbations of the global environment usually attributed to extraterrestrial causes (such as impact or radiation). Stepwise mass extinction[32-34,49] occurs as a series of discrete steps of highly accelerated or catastrophic extinction spread over 0.5–3.5 Myr intervals, each affecting only a portion of the global biota. Individual extinction steps may also be characterized, even predominantly, by ecological shock to surviving species manifested in abrupt population decline and/or restriction to refugia habitats; the latter reappear in recovery faunas as 'Lazarus taxa'[73]. In the well documented K/T, C/T and E/O events, extinction steps are ecologically graded from (first) stenotopic organisms (tropical reef biotas), proceeding through progressively more tolerant groups, to a final extinction of ecological generalists.

Proof of these hypotheses requires detailed (centimetre-scale) global stratigraphic analyses of extinction patterns among

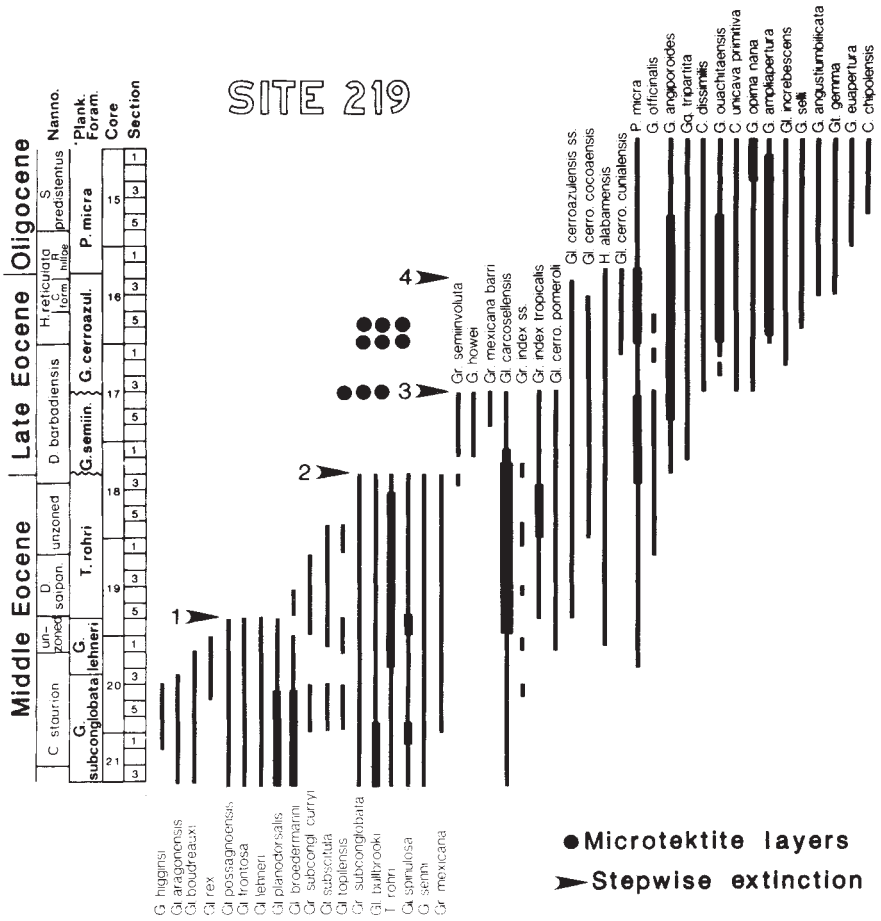

Fig. 4 Stepwise extinction pattern of planktonic foraminiferal species during the middle and late Eocene, DSDP Site 219, Indian Ocean. Wavy lines mark short hiatuses.

genetically and ecologically diverse taxa in the stages adjacent to mass extinctions. Such data are rare except among marine microbiotas: detailed macrobiotic data exist for the C/T and E/O boundaries of American and European basins, and for the K/T boundary only at a few Danish, Spanish, Texas and Mexican sites. We will show below that the data for these three mass extinctions support stepwise mass extinction theory.

Eocene–Oligocene boundary. *Stepwise extinctions of planktonic foraminifers.* Late Eocene strata provide the best opportunity for testing the relationship between a possible comet shower and a mass extinction because they contain three layers of microspherules of probable impact origin[27-29]. Several discrete intervals, or steps, of accelerated species extinctions of planktonic foraminifers extend from late middle Eocene to the Eocene-Oligocene boundary and include the period during which the microspherule layers were deposited. The interval during which these extinctions took place has been estimated at ~3.6 Myr[74], but new dates suggest that it may have been as brief as 1 Myr[75].

Analysis of more than 20 deep-sea cores shows that global stepwise extinctions of planktonic foraminifers involving four to six species at each step occurred during four very short intervals (Fig. 4; refs 32-34). In contrast, background extinctions occur at a rate of <1 species per Myr. Extinction steps are often associated with carbonate dissolution, representing condensed intervals where part of the record may be missing. Nevertheless, the extinction steps can be observed globally. Two of the extinction steps occurred in the very late middle Eocene and at the middle/late Eocene boundaries respectively, during which warm-water spinose middle Eocene species of foraminifers, comprising 60–70% of the microfaunal assemblages, became extinct successively. In each step, the vacated niches were subsequently occupied primarily by temperate-water marine species, along with an increasing abundance of cooler-water species. These extinctions are interpreted to be the result of rapid, short-term global climatic cooling, as supported by oxygen isotope data[32-34].

A third extinction step followed deposition of the earliest microspherule layer, near the top of the *Globigerapsis semiinvoluta* zone (Fig. 5). An iridium anomaly is present at this microspherule layer, and carbonate is reduced from 87% to 43%[27-29]. The *Globigerapsis* group permanently declined from ~50% to 1% of the foraminiferal fauna at this time and the four species of this group became extinct shortly thereafter. The ecological niche vacated by the decline of this group was occupied by expanding populations of the cooler-water *Globigerina linaperta-angiporoides* group.

The two closely spaced microspherule layers in the *Globorotalia cerroazulensis* zone are also associated with strong carbonate dissolution (Fig. 5), and a major iridium anomaly occurs at the second layer[27-29,35,36]. Five radiolarian species extinctions coincide with the second microspherule layer[38]. No foraminiferal or radiolarian species extinctions are associated with the third layer but there is a strong faunal response towards cooler populations at this time, presumably in response to continued climatic cooling (Fig. 5). The final extinction step occurred at the Eocene/Oligocene boundary[32-34], and is the least severe of the four. Although it involves the extinction of four species, these represent <5% of the individuals of the total foraminiferal population.

The foraminiferal data clearly show four stepwise intervals of accelerated species extinctions, but only one step can be directly related to an impact event. Five radiolarian species extinctions are related to a second impact event. Thus, at least two of the three impact events may have caused changes in the environment that ultimately led to the demise of ecologically sensitive species. Moreover, each of the three impact glass horizons is associated with low carbonate content. This may be

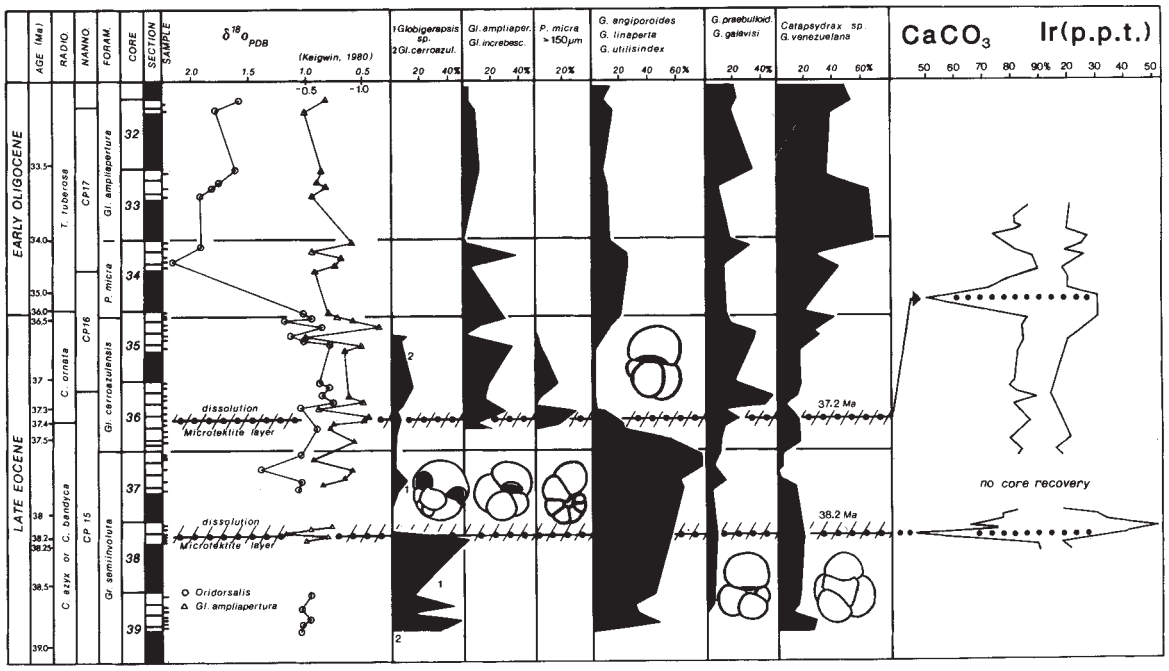

Fig. 5 Microtektite layers, per cent $CaCO_3$, iridium, oxygen isotope data and species abundance changes during the late Eocene to early Oligocene in the western equatorial Pacific DSDP Site 292.

partly due to global cooling or decreased productivity, and/or acid rain due to major impact events[76,77], but it is very difficult to separate the effects of a productivity change from those of dissolution; further studies are necessary to elucidate this relationship. Middle to late Eocene stepwise extinctions result from multiple causes, as there is no evidence of impacts associated with the two steps preceding or that following the deposition of the presently known impact glass layers.

Stepwise extinctions of molluscs. Gulf Coast molluscan data compiled from the field and literature show extinction patterns across the Eocene/Oligocene boundary that also support the concept of a stepwise mass extinction. Molluscan radiation in the middle Eocene reached its peak of species diversification in the Cook Mountain Formation (384 gastropod and bivalve species) and the overlying Gosport Formation (385 species), and then declined dramatically through a series of three discrete extinction events, two of them major, which occur between the middle/late Eocene and the Eocene/Oligocene boundaries.

The initial extinction event occurred just below the middle/late Eocene boundary, near the stratigraphic boundary between the Gosport and the Moody's Branch formations. Species extinctions across this boundary were 89% for gastropods (233 of 263 species) and 84% for bivalves (102 of 122 species). This extinction event corresponds to step 2 (Fig. 4) of the planktonic foraminiferal extinctions discussed above. A second step accelerated molluscan extinction took place near the top of the Moody's Branch Formation and equivalent strata. This extinction event lies within the early late Eocene (within planktonic foraminiferal zone P15; *Globigerapsis semiinvoluta* biozone). Species extinctions across this boundary were 72% for gastropods (139 of 193 species) and 63% for bivalves (50 of 80 species). This extinction event may be associated with step 3 (Fig. 4) of the planktonic foraminiferal extinctions observed in deep-sea sediments. The final extinction event occurred at the Eocene/Oligocene boundary among already depleted Gulf Coast molluscan faunas, with a loss of 58 of 60 gastropod species (97%) and 23 of 26 bivalve species (89%). Most of these species disappeared in the upper half of the Yazoo Formation, but the exact stratigraphic location of the extinction has not yet been determined. The extinction took place within 1 Myr or less.

Among mollusca, bivalves and planktonic foraminifera, warm-water genera suffered a higher specific extinction rate than cool-tolerant forms in the late Eocene/Oligocene boundary stepwise mass extinctions; in the middle late Eocene stepwise mass extinctions this was true for planktonic foraminifera. But macroinvertebrates show no clearly defined trends for the terminal Gosport event other than the greater effect on Gastropoda than on Bivalvia and the indiscriminate extinction of a broad range of genetic and ecological groups (see ref. 78 for a more detailed account).

Cretaceous/Tertiary boundary. Because of erosion or non-deposition due to sea-level lowering during the Cretaceous/Tertiary boundary interval, few sections preserve a record of mass extinction among shallow-water invertebrates during this time[47]. Most marine macrofaunal data are from Danish and Spanish sequences in shelf chalk facies[40,49,79–81]. Data from siliciclastic shelf facies are available from Texas[82], Mexico and Brazil[47,83]. Tethyan carbonate platform sequences in Jamaica[47,49,81,85], Puerto Rico, the Spanish Pyrenees[47,86,87] and the Middle East document collapse of the Cretaceous reef ecosystem below the K/T boundary. A composite analysis of the data suggests that one or more extinction steps preceded the main K/T extinction event.

The most prominent precursory extinction event occurred within the lower part of the Upper Maastrichtian *Abathomphalus mayaroensis* zone and follows Lower Maastrichtian diversification of Cretaceous marine biotas[49]. This event decimated specialized ammonites[47,81,88,81], diverse suspension-feeding deep-water benthos[47] and most tropical stenotopic reef-forming groups[47,49,85–87]. The extinction step is most dramatically seen in the tropical Caribbean data[84], where all 24 genera and 83 species of rudistids (reef-building bivalves) that were present near the Lower/Upper Maastrichtian boundary disappeared with the lower *A. mayaroensis* zone, even though mollusc-rich shallow carbonate platform environments persisted into the Palaeocene. A similar extinction pattern is suggested in Spanish and Middle Eastern data[47,86,87]. Only a single rudistid specimen, belonging to a eurytopic temperate-tropical group, is known at the K/T boundary (in Denmark)[90].

In addition to this clearly documented first step, there are

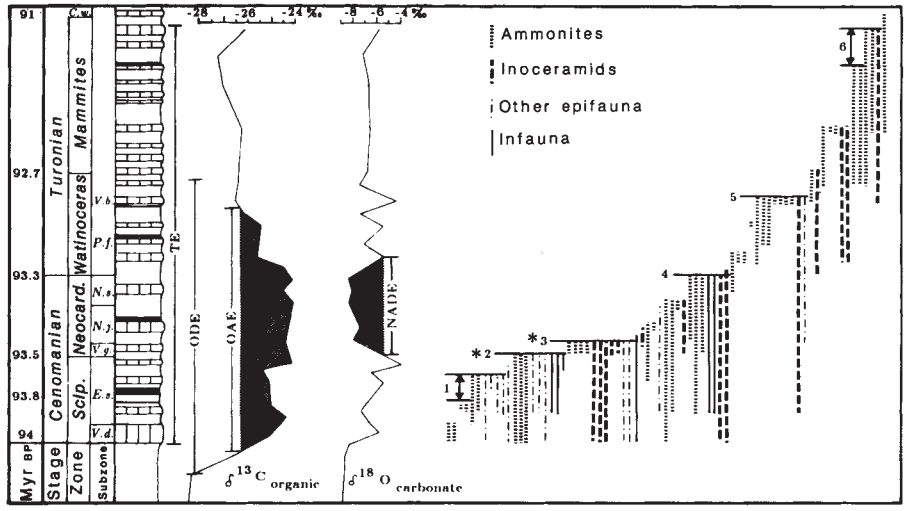

Fig. 6 Composite plot of the ranges of molluscan species in the western interior of the United States having last occurrences in the Cenomanian–Turonian boundary interval. The data are integrated from numerous sections, calibrated to individual volcanic ash (bentonite) and Milankovitch climate cycle strata, and are plotted against the western interior standard reference section (left) at Rock Canyon anticline near Pueblo, Colorado[103]. The $\sigma^{13}C_{organic}$ and $\sigma^{18}O_{carbonate}$ values (relative to PDB) are from the same section[106]. Species ranges are a graphic composite from stratigraphic sections analysed by Elder[103,104], and from range data of Koch[113,114], Cobban and Scott[115] and Cobban[123]. Biostratigraphic zones and subzones, in ascending order, are: the *Vascoceras diartianum* (*V.d.*) and *Euomphaloceras septemseriatum* (*E.s.*) subzones of the *Sciponoceras gracile* biozone (*Scip.*); the *Vascoceras gamai* (*V.g.*), *Neocardioceras juddi* (*N.j.*) and *Nigericeras scotti* (*N.s.*) subzones of the *Neocardioceras juddi* biozone (*Neocard.*); the *Pseudaspidoceras flexuosum* (*P.f.*) and *Vascoceras birchbyi* (*V.b.*) subzones of the *Watinoceras* biozone; the *Mammites nodosoides* biozone; and the *Collignoniceras woollgari* (*C.w.*) biozone. Numbered horizontal lines or intervals mark the possible stepwise extinctions; those marked by an asterisk denote major, well-documented extinction steps recognizable at most localities. Approximately 15 additional, mostly infaunal taxa (not plotted) are known to range through the entire interval, and many other species are either too rare or their taxonomy is too poorly known to determine their ranges accurately.

preliminary suggestions that a second and third extinction step may have preceded the end of the Maastrichtian. The possible second step[49] is in the middle of the *Abathomphalus mayaroensis* biozone, and its principal victims were the last generalized framework-building rudistids (Radiolitidae, Hippuritidae), characteristic inoceramid bivalves, generalized deep-water benthic macroinvertebrates and mid-water ammonite lineages[47,81,88,91]. The possible third precursory step, only 0.05–0.1 Myr before the main boundary extinction, is suggested by a short-term decline in specialized calcareous plankton[92–97], losses among deep-water shelled benthos, and extinction of the last giant solitary rudistids (*Titanosarcolites*) and the remaining ammonites (Denmark excepted)[91].

The biggest extinction step occurred at the Cretaceous/Tertiary boundary, and is marked by the near-simultaneous global extinction of most calcareous and siliceous oceanic plankton[92–96], diverse brachiopods[40,98], bryozoans[79,99] and molluscs[90], and terminal loss of 'endangered species' among already-decimated, typical Cretaceous groups (such as rudists, ammonites and inoceramid bivalves). This extinction event is associated with the large iridium anomaly, shocked mineral grains and other evidence for impact at the K/T boundary[40]. A 0.05 Myr interval characterized by small, depauperate, ecologically generalized basal Palaeocene biotas followed this end-Cretaceous extinction; this was succeeded within stabilizing marine environments (refs 81, 92–96, 100 and Fig. 1 of ref. 101) by rapid radiation among new and surviving Lower Palaeocene taxa and a return of 'Lazarus taxa'[73] from as yet undiscovered refugia.

Published plots of data from Denmark[40,49,98,99] suggest several more extinction steps among Lower Palaeocene bryozoa[99] and brachiopod species[40,98] up to 0.25 Myr above the K/T boundary, but these apparent extinction steps seem to coincide closely with the tops of samples spaced $\geq$1 m apart. We conclude that the sampling of the Danish Palaeocene is not yet sufficiently detailed to determine whether further extinction steps occur above the Cretaceous/Tertiary boundary.

Thus, one strong extinction step precedes the Cretaceous/Tertiary boundary, and others are suggested by existing data. More detailed (centimetre-scale) studies of the best available sections will be required in order to test whether other steps occurred.

Cenomanian/Turonian boundary. The Cenomanian/Turonian (C/T) mass extinction occurred near a high-stand of global eustatic sea level and broad amelioration of global climates. Four extraordinary environmental perturbations account for the unusual magnitude of the marine faunal extinction (30% of genera[42] and >70% of species)[47,103,104,113–117] in the C/T boundary interval (see Fig. 6): (1) the Bonarelli oceanic anoxic event (OAE)[10], represented worldwide by organic-rich, laminated shales, bituminous limestones[47,103,104], or by widespread deep-sea carbonate dissolution; (2) the lowering of average oceanic water temperatures[105], coupled with a rapid multi-stage temperature rise in shallow temperate seas (TE)[105–107], thus altering marine thermal regimes and enhancing density stratification; (3) a desalination event, lasting ~0.2 Myr, in the shallow, normal-marine, epicontinental seas of North America (NADE[106]) near peak eustatic high-stand, implying regionally extensive rainfall; and (4) a 1.5-Myr-long interval of massive destabilization of the global climate and ocean systems (ODE), indicated by abnormally rapid (50–100 kyr) large-scale fluctuations in the stable isotopes of carbon and oxygen[106,108,109]. The unusual rate, magnitude and character of these environmental perturbations may be impact-induced, but the evidence is inconclusive. A modest iridium anomaly just below the Cenomanian/Turonian boundary is suggested from North American and European data (C. J. Orth and F. Asaro, personal communication), but needs further verification. Two major impact craters (Steen River and Logoisk) have isotopic ages with uncertainties that encompass the Cenomanian/Turonian boundary interval[52,110].

The C/T mass extinction occurred over a 2.5 Myr interval (Fig. 6), and is characterized by brief intervals of highly accelerated extinction separated by longer recovery intervals with lower background extinction rates[47,103,104,107]. Two major molluscan extinction steps are globally recognizable in the C/T extinction interval (events 2, 4; Fig. 6) and are widely defined by the extinction of common taxa at many sections in North America. Four other extinction steps may also be present (events 1, 3, 5, 6; Fig. 6; but these are based on composite ranges of less common and more geographically restricted taxa. Following a buildup of subtropical-warm temperature diversity during the late Cenomanian rise in sea level, the initiation of the Bonarelli OAE, a global shift in ^{13}C abundance[106] and early phases of oceanic temperature decline (coupled with rapid temperature increases in temperate epicontinental seas[105,107]) were associated with event 1 (Fig. 6), in which a major loss of keeled planktonic foraminifera (*Rotalipora* lineage)[111,112] and a modest molluscan extinction occurred within 0.05–0.1 Myr[103,104].

The first major C/T molluscan extinction (event 2, Fig. 6) occurred within a 0.05 Myr interval at the top of the *S. gracile*

biozone (93.5 Myr), when accelerated thermal and chemical fluctuations in the marine realm (Fig. 6) and initiation of a large reduction in marine salinity in the North American Seaway ~0.3 Myr below the C/T boundary (NADE, Fig. 6) caused a 15–30% loss of genera in the central interior seaway[103,104,107,111] and a cumulative loss of 78–80% of molluscan species for extinction steps 1 and 2[113–115]. A brief oxygenation and recolonization event followed in warm epicontinental seas during the Bonarelli OAE and was ended by environmental perturbations associated with renewed regional oxygen depletion at event 3 (Fig. 6)[47,103,104].

A few surviving generalized molluscan and foraminiferal lineages persisted through the peak Bonarelli OAE before becoming abruptly extinct at the second major extinction (event 4, Fig. 6), coincident with peak excursions of the $\delta^{18}O$ and σ^{13C} curves (Fig. 6)[106]. This extinction event marks the biostratigraphically defined C/T boundary[116], and is equivalent to a nannofossil biozone boundary in the western interior of North America (ref. 117). Following a 50-kyr-long Lower Turonian anoxic interval (latest Bonarelli OAE) with virtually no benthic fauna, diverse warm-water biotas were repeatedly re-established, and then rapidly annihilated at events 5 and 6 (Fig. 6). The upper of these events coincided with the initiation of rapid global eustatic sea-level fall and the cooling of epicontinental seas, and was coupled with the last big stable-isotope excursions before the establishment of normal temperature marine conditions (Fig. 6).

Thus, several discrete extinction steps span the C/T boundary and appear to have been associated with extraordinary climatic, temperature and oceanic perturbations. These oscillations, acting on a global biota narrowly adapted to warm, equable, maritime-dominated climates, appear to be the direct cause of stepwise extinction; they may have been driven by extraterrestrial forcing.

Conclusions

We have presented three independent pieces of evidence supporting a connection between comet showers and clustering in terrestrial cratering and mass extinctions.

From the astronomical side, observations of comets have led to the theory of a comet cloud (the Oort cloud) surrounding the planetary system at a large distance from the sun; we calculate the temporal profile of a comet shower triggered by a star passing through the Oort cloud. From the geological side, four weak peaks are found in the age of distribution of impact craters over the past 100 Myr, as well as two compact clusters of ages of impact glass broadly coincident with crater-age peaks. From the palaeontological side, recent observations indicate a stepwise character for some well-documented mass extinctions in the past 100 Myr which roughly coincide with three of the four peaks in crater ages and which have a duration compatible with comet shower predictions.

It is too early to predict whether the hypotheses of comet showers will offer a general and global explanation for any or all mass extinctions. We enteratin a spectrum of differing opinions on this question, but the evidence cited here is suggestive of a causal connection in at least some cases.

Definitive testing of this hypothesis will require a new level of detailed inquiry in each of the relevant fields. From orbital dynamics we need a deeper understanding of the frequency and intensity of comet showers and of the pattern of impacts to be expected from the range of possible disturbances of the Oort cloud and from non-shower, random events. From impact geology we need a more complete catalogue of terrestrial craters and more refined dating of these structures. A useful test, the dating of a large sample of lunar craters, must unfortunately wait for the indefinite future. Physical and chemical stratigraphers must search for evidence of impact (iridium, tektites and microspherules, shocked mineral grains) at 1–10-cm intervals throughout large portions of the stratigraphic record. Biostratigraphers must document at very high resolution the fine structure of mass extinction intervals, a task complicated by the necessity, in many cases, of dealing with the statistics of small samples. Ocean and climate modelling will eventually be necessary to understand the effects of multiple impacts on the biosphere. The intriguing results obtained to date suggest that this will be a worthwhile enterprise.

We acknowledge interesting discussions with F. Asaro, L. Alvarez, R. Carlson, H. Michel, A. Montenari and R. Muller. Part of this work was supported by the NASA Planetary Geology and Geophysics Program and was performed at the Jet Propulsion Laboratory under contract with NASA. Part was supported by the Alfred P. Sloan Foundation (P.H.) and the National Science Foundation (P.H., W.A., T.H. and E.G.K.).

1. Wetherill, G. W. & Shoemaker, E. M. *Spec. Pap. geol. Soc. Am.* **190,** 1-13 (1982).
2. Hills, J. G. *Astr. J.* **86,** 1730-1740 (1981).
3. Muller, R. A. in *The Search for Extraterrestrial Life: Recent Developments* (ed. Papagiannis, S.) 233-243 (Reidel, Dordrecht, 1985).
4. Alvarez, L. W., Alvarez, W., Asaro, F. & Michel, H. V. *Science* **208,** 1095-1108 (1980).
5. Orth, C. J. *et al. Science* **214,** 1341-1343 (1981).
6. Alvarez, W., Alvarez, L. W., Asaro, F. & Michel, H. V. *Spec. Pap. geol. Soc. Am.* **190,** 305-315 (1982).
7. Luck, J. M. & Turekian, K. K. *Science* **222,** 613-615 (1983).
8. Kastner, M., Asaro, F., Michel, H. V., Alvarez, W. & Alvarez, L. W. *Science* **226,** 137-143 (1984).
9. Smit, J. & Klaver, G. *Nature* **292,** 47-49 (1981).
10. Montanari, A. *et al. Geology* **11,** 668 (1983).
11. Smit, J. & Kyte, F. T. *Nature* **310,** 403-405 (1984).
12. Bohor, B. F., Foord, E. E., Modreski, P. J. & Triplehorn, D. M. *Science* **224,** 867-869 (1984).
13. Izett, G. A. & Pillmore, C. L. *Geol. Soc. Am. Abstr. Prog.* **17,** 617 (1985).
14. Bohor, B. F., Modreski, P. J., Foord, E. E. *Lunar planet. Sci. Conf. Abstr.* **16,** 79 (1985).
15. Wolbach, W. S., Lewis, R. S. & Anders, E. *Science* **230,** 167-170 (1985).
16. Jones, E. M. & Kodis, J. W. *Spec. Pap. geol. Soc. Am.* **190,** 175-186 (1982).
17. Mclean, D. M. *Syllogeus* **39,** 143-144 (1982).
18. Mclean, D. M. *Eos* **64,** 245 (1983).
19. Mclean, D. M. *Cretac. Res.* **6,** 235-259 (1985).
20. Officer, C. B. & Drake, C. L. *Science* **219,** 1383-1390 (1983).
21. Officer, C. B. & Drake, C. L. *Science* **227,** 1161-1167 (1985).
22. Officer, C. B., Hallam, A., Drake, C. L. & Devine, J. D. *Nature* **326,** 143-149 (1987).
23. Alvarez, W., Alvarez, L. W., Asaro, F. & Michel, H. V. *Science* **223,** 1183-1186 (1984).
24. Alvarez, W. *Eos* **67,** 653 (1986).
25. Ngo, H. H., Wasserburg, G. J. & Glass, B. P. *Geochim. cosmochim. Acta* **49,** 1429-1485 (1985).
26. Glass, B. P., Burns, C. A., Crosbie, J. R. & DuBois, D. L. *Proc. lunar planet. Sci. Conf.* **16,** D175 (1985).
27. Keller, G. *et al. Meteoritics* (in the press).
28. Keller, G., D'Hondt, S. & Vallier, T. L. *Science* **221,** 150-152 (1983).
29. D'Hondt, S., Keller, G. & Stallart, R. S. *Meteoritics* (in the press).
30. Glass, B. P. & Zwart, M. J. *Geol. Soc. Am. Bull.* **90,** 595-602 (1979).
31. Glass, B. P. & Crosbie, J. R. *Bull. Am. Ass. Petrol. Geol.* **66,** 471-476 (1982).
32. Keller, G. *Mar. Micropaleont.* **7,** 463-486 (1983).
33. Keller, G. *J. Paleont.* **59,** 882-903 (1985).
34. Keller, G., *Mar. Micropaleont.* **10,** 267-293 (1986).
35. Alvarez, W., Asaro, F., Michel, H. V. & Alvarez, L. W. *Science* **216,** 886-888 (1982).
36. Ganapathy, R. *Science* **216,** 885-886 (1982).
37. Glass, B. P., DuBois, D. L. & Ganapathy, R. *J. Geophys. Res.* **87,** 425-428 (1982).
38. Sanfilippo, A., Reidel, W. R., Glass, B. P. & Kyte, F. T. *Nature* **314,** 613-615 (1985).
39. Archibald, J. D. & Clemens, W. A. *Am. Scient.* **70,** 377-385 (1982).
40. Alvarez, W. *et al. Science* **223,** 1135-1141 (1984).
41. Fischer, A. G. & Arthur, M. A. *Spec. Publs. Soc. econ. Paleont. Min.* **25,** 19-50 (1977).
42. Raup, D. M. & Sepkoski, J. J. *Proc. natn. Acad. Sci. U.S.A.* **81,** 801-805 (1984).
43. Davis, M., Hut, P. & Muller, R. A. *Nature* **308,** 715-717 (1984).
44. Whitmire, D. P. & Jackson, A. A. *Nature* **308,** 713-715 (1984).
45. Rampino, M. R. & Stothers, R. B. *Nature* **308,** 709-712 (1984).
46. Muller, R. A. in *The Galaxy and the Solar System* (eds Smoluchowski, R., Bahcall, J. N. & Matthews, M.) 387-396 (Univ. Arizona Press, Tucson, 1986).
47. Kauffman, E. G. in *Catastrophes and Earth History, The New Uniformitarianism* (eds Berggren, W. A. & Van Couvering, J. A.) 151 (Princeton Univ. Press, 1984).
48. Kauffman, E. G. in *Fine-Grained Deposits and Biofacies of the Cretaceous Western Interior Seaway: Evidence of Cyclic Sedimentary Processes* (eds Pratt, L. M., Kauffman, E. G. & Zelt, F. B.) IV-XI (Soc. Econ. Paleontol. Mineralog., Tulsa, 1985).
49. Kauffman, E. G. in *Lecture Notes in Earth Sciences,* Vol. 8 (ed. Walliser, O. H.) 279 (Springer, New York, 1986).
50. Raup, D. M. *Science* **231,** 1528-1533 (1986).
51. Raup, D. M. & Sepkoski, J. J. *Science* **231,** 833-836 (1986).
52. Alvarez, W. & Muller, R. A. *Nature* **308,** 718-720 (1984).
53. Shoemaker, E. M. & Wolfe, R. F. *Meteoritics* **19,** 313 (1984).
54. Whitmire, D. P. & Matese, J. J. *Nature* **313,** 36-38 (1986).
55. Tremaine, S. D. in *The Galaxy and the Solar System* (eds Smolochowski, R., Bahcall, J. N. & Matthews, M.) 409-416 (Univ. Arizona Press, Tucson, 1986).
56. Delsemme, A. H. in *Comets* (ed. Wilkening, L. L.) 85-130 (Univ. Arizona Press, Tucson, 1982).
57. Palme, H. *Spec. Pap. geol. Soc. Am.* **190,** 223-233 (1982).
58. Asaro, F. *Syllogeus* **39,** 6-9 (1982).
59. Heisler, J. & Tremaine, S. *Icarus* **65,** 13-26 (1986).
60. Weissman, P. R. *Space Sci. Rev.* **41,** 299-349 (1985).
61. Shoemaker, E. M. & Wolfe, R. F. *Lunar planet Sci.* **15,** 780-781 (1984).
62. Fernández, J. A. & Ip, W.-H. *Icarus* (submitted).
63. Weissman, P. R. in *Dynamics of the Solar System* (ed. Duncombe, R. L.) 277-282 (Reicel, Dordrecht, 1979).
64. Weissman, P. R. thesis, Univ. California Los Angeles (1978).
65. Hut, P. *Nature* **311,** 638-640 (1984).

66. Hills, J. G. *Nature* **311**, 636–638 (1984).
67. Wetherill, G. W. *Bull. Am. astr. Soc.* **18**, 763 (1986).
68. Shoemaker, E. M. & Wolfe, R. F. in *The Galaxy and the Solar System* (eds Smoluchowski, R., Bahcall, J. N. & Matthews, M.) 338–386 (Univ. Arizona Press, Tucson, 1986).
69. Glass, B. P., R. Swincki, M. B. & Zwart, P. A. *Proc. lunar planet. Sci. Conf.* **10**, 2535 (1979).
70. Storzer, D. & Wagner, G. A. *Naturwissenschaften* **67**, 90–91 (1980).
71. Storzer, D., Jessberger, E. K., Klay, N. & Wagner, G. A. *Meteorites* **19**, 317 (1984).
72. Glass, B. P. *Earth planet. Sci. Lett.* (submitted).
73. Flessa, K. W. & Jablonski, D. *Paleobiology* **9**, 315–321 (1983).
74. Berggren, W. A., Kent, D. V. & Flynn, J. J. *Geol. Soc. Lond. spec. Pap.* (in the press).
75. Montanari, A. *et al. Geology* **13**, 596–599 (1985).
76. Prinn, R. G. *Eos* **66**, 813 (1985).
77. Lewis, Z. S., Watkins, G. H., Hartman, H. & Prinn, R. G. *Spec. Pap. geol. Soc. Am.* **190**, 215–221 (1982).
78. Hansen, T. A. *Palaios* (in the press).
79. Birkeland, T. & Bromley, R. G. (eds) *Cretacious–Tertiary Boundary Events: Symposium 1, The Maastrichtian and Danian of Denmark* (Univ. Copenhagen, 1979).
80. Christensen, W. K. & Birkeland, T. (eds) *Cretacious–Tertiary Boundary Events: Symposium 2, Proceedings* (Univ. Copenhagen, 1979).
81. Mount, J. F., Margolis, S. V., Showers, W., Ward, P. & Doehne, E. *Palaios* **1**, 87–92 (1986).
82. Hansen, T. A., Farrand, R., Montgomery, H. & Billman, H. in *The Cretaceous–Tertiary Boundary and Lower Tertiary of the Brazos River Valley* (ed. Yancey, T. E.) 21–36 (Am. Assn. Pet. Geol., Texas, 1984).
83. Mabesoone, J. M., Tinoco, I. M. & Coutinho, P. N. *Palaeogeogr. Palaeoclimatol. Palaeoecol.* **4**, 161–185 (1968).
84. Kauffman, E. G. & Johnson, C. C. *Science* (submitted)
85. Kauffman, E. G. & Sohl, N. F. *Verh. Naturf. Ges. Basel* **84**, 399–467 (1974).
86. Liebau, A. *Proc. Colloq. Eur. Micropalaeont.* **13**, 3–28 (1973).
87. Liebau, A. *Neues Jb. Geol. Palaeone*, **157**, 233–237 (1978).
88. Wiedmann, J. *Estud. Geol.* **20**, 107–148 (1964).
89. Ward, P., Wiedmann, J. & Mount, J. F. *Geology* **14**, 899–903 (1986).
90. Heinberg, C. in *Cretaceous–Tertiary Boundary Events: Symposium 1, The Maastrichtian and Danian of Denmark* (eds Birkelund, T. & Bromley, R. G.) 58 (Univ. Copenhagen, 1979).
91. Birkelund, T. in *Cretaceous–Tertiary Boundary Events: Symposium 1, The Maastrichtian and Danian of Denmark* (eds Birkelund, T. & Bromley, R. G.) 51–57 (Univ. Copenhagen, 1979).
92. Smit, J. *Spec. Pap. geol. Soc. Am.* **190**, 329–352 (1982).
93. Perch-Nielsen, K., McKenzie, J., Quziang, H. *Spec. Pap. geol. Soc. Am.* **190**, 353–371 (1982).
94. Thierstein, H. *Spec. Pap. geol. Soc. Am.* **190**, 385–399 (1982).
95. Thierstein, H. *Spec. Publs. Soc. econ. Paleont. Miner.* **32**, 355–394 (1981).
96. Thierstein, H. R. & Okada, H. in *Init. Rep. DSDP* **43**, 601–616 (1979).
97. Herm, D. *Deutsche Geol. Ges. Zeitschur. Jahrg.* **15**, 277–348 (1963).
98. Surlyk, F. & Johannsen, M. D. *Science* **233**, 1174–1177 (1984).
99. Birkelund, T. & Hakansson, E. *Spec. Pap. geol. Soc. Am.* **190**, 373–384 (1982).
100. Boersma, A. & Shackleton, N. J. *Init. Rep. DSDP* **62**, 513–526 (1981).
101. Smit, J. & van der Kaars, S. *Science* **223**, 1177–1179 (1984).
102. Arthur, M. A. & Schlanger, S. O. *Bull. Am. Ass. Petrol. Geol.* **63**, 870–885 (1979).
103. Elder, W. P. in *Fine-Grained Deposits and Biofacies of the Cretaceous Western Interior Seaway: Evidence of Cyclic Sedimentary Processes* (eds Pratt, L. M., Kauffman, E. G. & Zelt, F. B.) 157–169 (Soc. Econ. Paleontol. Mineralog., Tulsa, 1985).
104. Elder, W. P. thesis, Univ. Colorado (1987).
105. Kauffman, E. G. in *Treatise on Invertebrate Paleontology*, Pt A (eds Robinson, R. A. & Teichert, C.) 418 (Geol. Soc. Am., Univ. Kansas Press, 1978).
106. Pratt, L. M. in *Fine-Grained Deposits and Biofacies of the Cretaceous Western Interior Seaway: Evidence of Cyclic Sedimentary Processes* (eds Pratt, L. M., Kauffman, E. G. & Zelt, F. B.) 38 (Soc. Econ. Paleontol. Mineralog., Tulsa, 1985).
107. Kauffman, E. G. *Geol. Ass. Can. spec. Pap.* **27**, 273–306 (1984).
108. Kauffman, E. G. *Geol. Soc. Am. Abstr. Progm.* **16**, 555 (1984).
109. Kauffman, E. G. & Hansen, T. *Eos* **66**, 46; 813 (1985).
110. Grieve, R. A. F. *Spec. Pap. geol. Soc. Am.* **190**, 25–37 (1982).
111. Leckie, R. M. in *Fine-Grained Deposits and Biofacies of the Cretaceous Western Interior Seaway: Evidence of Cyclic Sedimentary Processes;* (eds Pratt, L. M., Kauffman, E. G. & Zelt, F. B.) 139–150 (Soc. Econ. Paleontol. Mineralog., Tulsa, 1985).
112. Eicher, D. L. & Diner, R. in *Fine-Grained Deposits and Biofacies of the Cretaceous Western Interior Seaway: Evidence of Cyclic Sedimentary Processes* (eds Pratt, L. M., Kauffman, E. G. & Zelt, F. B.) 60–71 (Soc. Econ. Paleontol. Mineralog., Tulsa, 1985).
113. Koch, C. F. thesis, George Washington Univ. (1977).
114. Koch, C. F. *Paleobiology* **6**, 184–192 (1980).
115. Cobban, W. A. & Scott, G. R. *Prof. Pap. U.S. geol. Surv.* **645**, 108 (1972).
116. Birkelund, T. *et al. Bull. geol. Soc. Danm.* **33**, 1–108 (1984).
117. Watkins, D. K. in *Fine-Grained Deposits and Biofacies of the Cretaceous Western Interior Seaway: Evidence of Cyclic Sedimentary Processes* (eds Pratt, L. M., Kaufmann, E. G. & Zelt, F. B.) 151–156 (Soc. Econ. Paleontol. Mineralog., Tulsa, 1985).
118. Gentner, W., Kirsten, T., Storzer, D. & Wagner, G. A. *Earth planet. Sci. Lett.* **20**, 204–210 (1973).
119. McDougall, I. & Lovering, J. F. *Geochim. cosmochim. Acta* **33**, 1057–1070 (1969).
120. Storzer, D. & Wagner, G. A. *Meteoritics* **14**, 541–542 (1979).
121. Storzer, D. & Wagner, G. A. *Meteoritics* **12**, 368–369 (1977).
122. Storzer, D. *Meteoritics* **20**, 765–766 (1985).
123. Cobban, W. A. in *Fine-grained Deposits and Biofacies of the Cretaceous Western Interior Seaway: Evidence of Cyclic Sedimentary Processes* (eds Pratt, L. M., Kauffman, E. G. & Zelt, F. B.) 135–138 (Soc. Econ. Paleontol. Mineralog., Tulsa, 1985).

ARTICLES

Stratospheric trace gases in the spring 1986 Antarctic atmosphere

C. B. Farmer, G. C. Toon, P. W. Schaper, J.-F. Blavier & L. L. Lowes

Jet Propulsion Laboratory, California Institute of Technology, Pasadena, California 91109, USA

The atmospheric absorption features of over 500 infrared solar spectra recorded at McMurdo Station, have been analysed to determine the vertical column abundances of trace gases crucial to the understanding of the 'ozone hole' phenomenon.

SATELLITE measurements[1,2] have now established that the springtime ozone depletion, first reported by Farman *et al.*[3], extends throughout the polar vortex, a region of the atmosphere isolated by the polar circulation during the Antarctic winter and usually centred over eastern Antarctica. During September and October 1986, a period during which we monitored the atmosphere above McMurdo Station (78° S, 166° E), we were fortunate that we were near the centre of the ozone hole on two occasions; 15–22 September and 15–23 October. The edge of the hole, as defined by the maximum ozone gradient, was close to McMurdo on three occasions: 5–8 September, 23–28 September and 6–13 October. Thus, our observations sampled the polar atmosphere deep inside the vortex as well as the warmer regions close to the edge.

The observations were made with the JPL MkIV Interferometer, a high-resolution Michelson interferometer built specifically for recording atmospheric spectra from remote ground-based sites, aircraft and from stratospheric balloons. The instrument is double-passed with one fixed and one moving corner reflector, allowing a 200-cm maximum optical path difference. For the majority of the spectra recorded at McMurdo the maximum path difference of the scans was limited to 66 cm, giving an unapodized spectral resolution of 0.01 cm^{-1}. The carriage which holds the moving reflector is driven by a flexible integrating nut riding on a lead screw. This arrangement, together with the double-passed optical scheme, makes the instrument resistant to the effects of mechanical distortion and shock; this was especially important when operating under the conditions of wind and thermal stress encountered in the Antarctic environment. The spectral range of the instrument is covered by two detectors: an InSb detector is used for the shorter wavelengths (1.8–5.5 μm, 1,800–5,500 cm^{-1}) and a HgCdTe photoconductor for the range 5.5–15 μm (650–1,800 cm^{-1}). Both detectors are cooled to liquid nitrogen temperatures. The optical path difference between the two arms of the interferometer is monitored during the scan by a He–Ne laser whose interference fringes are used to trigger the sampling of the two signal channels. At the sampling rate of 10^4 s^{-1}, each pair of one million-point interferograms is recorded in 100 s.

An advantage of this technique is that the measurements of all of the constituents are made simultaneously in the same airmass, so that the results presented here represent self-contained inventories for each day. Due to the low solar angles, the stratospheric airmass sampled by our instrument was, at times, as much as 200 km away from the observation site, a point to remember when comparisons are made between these and other measurements made in slightly different airmasses.